High pressure study of the zinc phosphide semiconductor compound in two different phases

2009 J. Phys.: Condens. Matter 21 275802

(http://iopscience.iop.org/0953-8984/21/27/275802)

J. Phys.: Condens. Matter **21** (2009) 275802 (6pp) doi:10.1088/0953-8984/21/27/275802

High pressure study of the zinc phosphide semiconductor compound in two different phases

Ali Mokhtari

Simulation Laboratory, Department of Physics, Faculty of Science, Shahrekord University, PB 115, Shahrekord, Iran

E-mail: mokhtari@sci.sku.ac.ir

Received 19 March 2009, in final form 27 May 2009
Published 12 June 2009
Online at stacks.iop.org/JPhysCM/21/275802

Abstract

Electronic and structural properties of the zinc phosphide semiconductor compound are calculated at hydrostatic pressure using the full-potential all-electron linearized augmented plane wave plus local orbital (FP-LAPW + lo) method in both cubic and tetragonal phases. The exchange–correlation potential is treated by the generalized gradient approximation within the scheme of Perdew, Burke and Ernzerhof, GGA96 (1996 *Phys. Rev. Lett.* **77** 3865). Also, the Engel and Vosko GGA formalism, EV-GGA (Engel and Vosko 1993 *Phys. Rev.* B **47** 13164), is used to improve the band-gap results. Internal parameters are optimized by relaxing the atomic positions in the force directions using the Hellman–Feynman approach. The lattice constants, internal parameters, bulk modulus, cohesive energy and band structures have been calculated and compared to the available experimental and theoretical results. The structural calculations predict that the stable phase is tetragonal. The effects of hydrostatic pressure on the behavior of band parameters such as band-gap, valence bandwidths and internal gaps (the energy gap between different parts of the valence bands) are studied using both GGA96 and EV-GGA.

1. Introduction

Nitride, phosphide and arsenide compounds in II_3V_2 group semiconductors and their alloys have already been intensively investigated [1–13]. The photovoltaic and unusual transport properties cause considerable attention on these compounds. Among them, zinc phosphide was considered as early as the 1950s as one of the most promising low-cost and high-efficiency semiconductors for use as a photovoltaic solar energy converter [14].

Zinc phosphide is a polar and p-type semiconductor with mixed ionic–covalent bonds. This compound is crystallized in both the body centered cubic and the primitive tetragonal structures. The cubic structure is formed in the anti-bixbyite phase of the mineral $(Mn, Fe)_2O_3$ with a space group of T_h^7 (Ia_3). The second phase is tetragonal with a unit cell containing eight molecules with the space group belonging to D_{4h}^{15} $(P42/nmc)$ [15]. The experimental and theoretical works on the Zn_3P_2 compound are as follows.

The optical properties of bulk and thin-film zinc phosphide have been established by Fagen [7]. It was concluded that this material could be appropriate for use as the photon-absorbing and minority-carrier generating portion of a photovoltaic cell. The thin Zn_3P_2 films were grown on mica/Fe/Si substrates and their drift mobility were measured. Pawlikowski [8, 9] has investigated its absorption coefficient over a wide temperature range, and obtained 1.315 eV at 300 K and 1.335 eV within the temperature range 5–80 K for the energy gap. Optical vibrations in the Zn_3P_2 lattice were investigated by Misiewicz [10]. Solid solutions of the Cd_3P_2–Zn_3P_2 system have been prepared by direct melting and sintering methods and their physical properties have been measured [16]. Nelson and Kazmerski [17] have studied the ultraviolet photoemission of Zn_3P_2 utilizing synchrotron radiation to characterize changes in the valence band electronic structure as a function of annealing temperature. From 2004 to 2007, several experimental works on the bulk and thin film have been done [6–8]. Using the semi-empirical tight-binding method, a theoretical work has been carried out on Zn_3P_2 and its similar compounds [5].

To the best of our knowledge, there are no theoretical works exploring the structural and electronic properties of the cubic phase of this compound, and also no calculations based

Table 1. Internal parameters for cubic and tetragonal phases of Zn_3P_2.

	Parameters	Presented work	Exp. results [15, 25]
Tetragonal	u_1, v_1	0.283, 0.3818	0.283, 0.386
	u_2, v_2	0.2142, 0.1051	0.217, 0.103
	u_3, v_3	0.2465, 0.6456	0.250, 0.647
	w_1, w_2, w_3	0.2475, 0.2425, 0.2542	0.250, 0.239, 0.261
Cubic	x, y, z	0.392, 0.140, 0.370	—
	u	−0.0092	—

on the full-potential linearized augmented plane wave (FP-LAPW) method were performed for any phases of Zn_3P_2. The aim of this paper is a comparative study of physical properties of both phases of this compound at ambient condition and hydrostatic pressure.

The paper is organized as follows. Section 2 gives details of the computational method and some important parameters. Results and discussion concerning structural and electronic properties and the effect of hydrostatic pressure on the band parameters are in section 3. Section 4 summarizes the conclusions.

2. Theoretical framework

The self-consistent and first-principle calculations have been carried out using the scalar relativistic FP-LAPW + lo method, as implemented in the all electron WIEN2k code [18], within density functional theory (DFT) [19, 20]. The GGA96 [21], which is based on exchange–correlation energy optimization, is utilized to optimize the internal parameters and to calculate the total energy. The Engel–Vosko [22] generalized gradient approximation (EV-GGA), which optimizes the exchange–correlation potential, and also GGA96, are used for band structure calculations. In the FP-LAPW + lo approach the wavefunction, electron density and potential are differently expanded in two regions of the unit cell. Inside the non-overlapping spheres of radius R_{MT} around each atom, spherical harmonic expansion is used, and in the remaining space of the unit cell the plane wave basis set is chosen. The values of 2.3 and 1.9 au for Zn and P atoms respectively have been chosen for the muffin-tin radii. The maximum l value for the wavefunction expansion inside the atomic spheres is confined to $l_{max} = 10$. The basis set size is fixed by choosing $R_{MT} \times K_{max} = 7.5$, where R_{MT} is the smallest muffin-tin radius and K_{max} is the truncation for the modulus of the reciprocal lattice vector. The electron density is self-consistently determined using 11 and 12 k-points in the irreducible symmetry wedge of the Brillouin zone for cubic and tetragonal phases respectively. Convergence of total energies with respect to the number of k-points and K_{max} has been thoroughly checked. Convergence criteria for the energy and charge difference were 0.01 mRyd and 0.0001, respectively.

3. Results and discussion

3.1. Total-energy calculations

The Zn_3P_2 compound is crystallized in both cubic and tetragonal structures with the space group of T_h^7 (Ia_3) and D_{4h}^{15} ($P42/nmc$), respectively. In the tetragonal phase, the cation atoms (Zn) are located on four equally spaced planes perpendicular to the c axis, whereas the phosphorus atoms lie on parallel planes midway between two adjacent cation planes. The Zn atoms are in general positions, 8g, in three different groups: Zn1 (0, u_1, v_1; etc), Zn2 (0, u_2, v_2; etc) and Zn3 (0, u_3, v_3; etc). The phosphorus atoms are divided in three distinct groups at the special positions of 4c (0, 0, w_1; etc), 4d (0, 0.5, w_2; etc) and 8f (w_3, w_3, 0; etc).

Table 2. Lattice parameters, bulk modulus (B), its pressure derivative (B'), cohesive energy per formula unit, $E_{cohesive}$, minimum energy and mean value of bond length Zn–P obtained using FP-LAPW + lo calculations within GGA96 for Zn_3P_2 compounds. Results of others are included for comparison.

	Parameters	Presented work	Other results
Tetragonal	a, c (au)	15.374, 21.740	15.3013, 21.6377 [15, 25] [a]
	B (GPa)	72.89	—
	B'	4.44	—
	$E_{cohesive}$ (Ryd)	1.254	—
	Mean bond lengths	2.492	2.48 [24] [b]
Cubic	a (au)	21.674	—
	B (GPa)	71.63	—
	B'	4.34	—
	$E_{cohesive}$ (Ryd)	1.191	—
	Mean bond lengths	2.482	—

[a] Experimental.
[b] Tight-binding calculations.

The second structure crystallizes in the cubic anti-bixbyite phase of the mineral $(Mn, Fe)_2O_3$ compounds in the body centered space group of $T_h^7(206)$ with 40 atoms per primitive cell. In this structure, the metal atoms are in tetrahedral sites of a cubic close packed array of P atoms. The metal atoms are in general positions 48e of Ia_3 (x, y, z; etc), and there are two kinds of P atoms. P1 is in the position 8b (1/4, 1/4, 1/4; etc) and P2 is in the position 24d (u, 0, 1/4; etc) [15].

The available experimental lattice constants and internal parameters are used as the starting point to perform the structural calculations. As no calculated or experimental values for internal parameters of these compounds in the cubic phase have yet been reported in the literature, at first rough values for them are selected from similar compounds such as Be_3P_2 and Mg_3P_2. The internal parameters have been optimized by relaxing the atomic positions in the force direction using molecular dynamic methods. Then the optimized internal parameters are used to calculate the total energy for several lattice volumes, and by fitting the results with the Murnaghan equation of state [23] the equilibrium lattice parameters for each compound have been calculated. Finally, using the new optimized lattice parameter, once again more accurate values of internal parameters are re-calculated. The calculated lattice constant and internal parameters were then used to optimize the c/a ratio of the tetragonal cell with constant volume. The calculated equilibrium lattice constants, cohesive energy per formula unit, bulk modulus and its pressure derivative and internal parameters are reported in tables 1 and 2 for both phases and compared with other results.

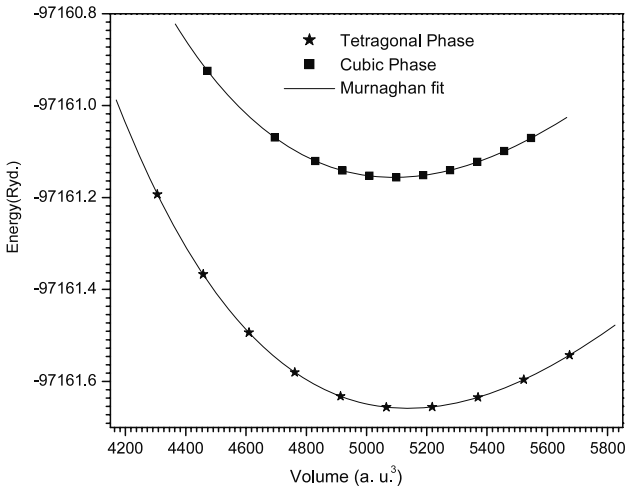

Figure 1. Calculated total energies (Ryd) as a function of primitive cell volume for the Zn_3P_2 compound in both cubic and tetragonal phases.

The cohesive energy is defined as the total energy of isolated atoms minus the energy of the formula unit in the solid. In order to obtain an accurate value for the cohesive energy, the energy calculations for isolated atoms and the crystal must be performed at the same level of accuracy. To fulfil such a requirement, the energy of an isolated atom was computed by considering a large cell containing just one atom. The size of this cube was chosen sufficiently large that the energy convergence with respect to the size of the cube was less than 0.001 Ryd. The corresponding sides were obtained as 21 and 25 au respectively for P and Zn atoms.

The noticeable points concerning these calculations are as follows.

The obtained lattice and internal parameters for the tetragonal phase are in good agreement with the available experimental values. The overestimations are obtained as about 0.46% and 0.47% for a and c parameters respectively, comparing to the experimental data. To our knowledge, no structural calculations have been reported for the cubic phase in the literature, hence our results can be considered as a prediction.

In spite of the atomic number of Zn being higher than those of Mg and Ca, the equilibrium volumes in both phases of zinc phosphide are smaller than the corresponding volumes in the similar compounds Mg_3P_2 and Ca_3P_2 [4]. This result is due to the fact that the electrons in s and p orbitals are screened by the fully occupied d orbital of the Zn atom. Therefore, the bond length and equilibrium volume will be small.

Total energy versus volume of the primitive cell is shown for both phases in figure 1. It is evident that the more stable structure is in the tetragonal phase, consistent with the obtained values of the cohesive energies of both phases. It should be noted that the cubic phase is formed by increasing the temperature of the tetragonal phase, not by exerting pressure on it.

3.2. Electronic properties

It is well known that the LDA and the GGA usually underestimate the energy band-gap [26, 27]. This is mainly due to the fact that they have simple forms that are not sufficiently flexible for accurately reproducing both the exchange–correlation energy and its electron density derivative. Engel and Vosko [22] by considering this shortcoming constructed a new functional form of the GGA which was able to better reproduce the exchange potential at the expense of less

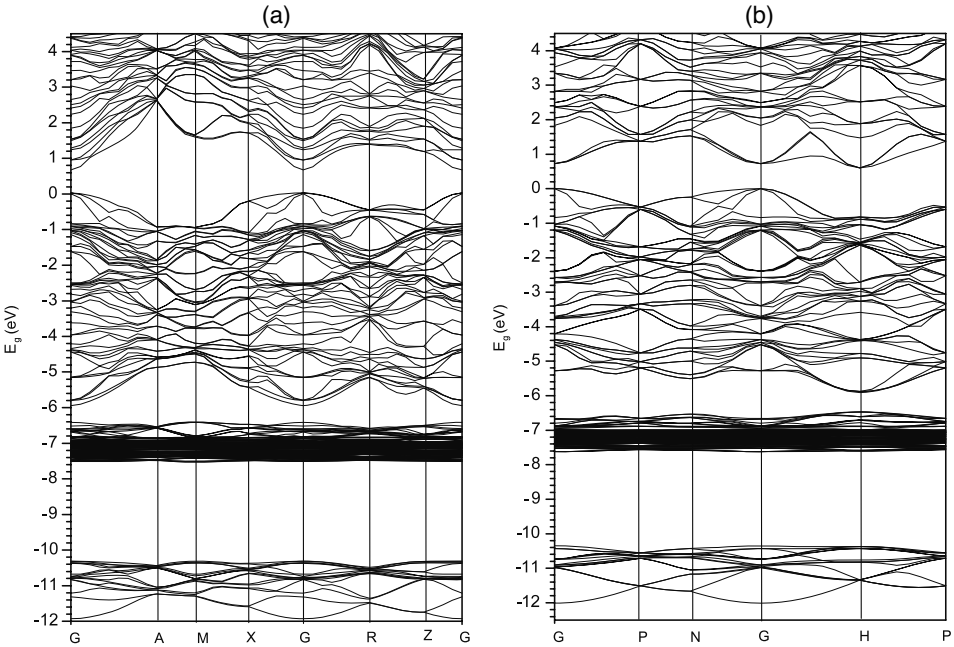

Figure 2. Band structures of Zn_3P_2 compounds obtained by EV-GGA at theoretical equilibrium lattice constants calculated by GGA96: (a) tetragonal phase, between $G(0, 0, 0)$, $A(1/2, 1/2, 1/2)$, $M(1/2, 1/2, 0)$, $X(1/2, 0, 0)$, $R(1/2, 0, 1/2)$ and $Z(0, 0, 1/2)$ symmetry points; (b) between $G(0, 0, 0)$, $P(1/4, 1/4, 1/4)$, $N(0, 0, 1/2)$ and $H(1/2, 1/2, -1/2)$ points.

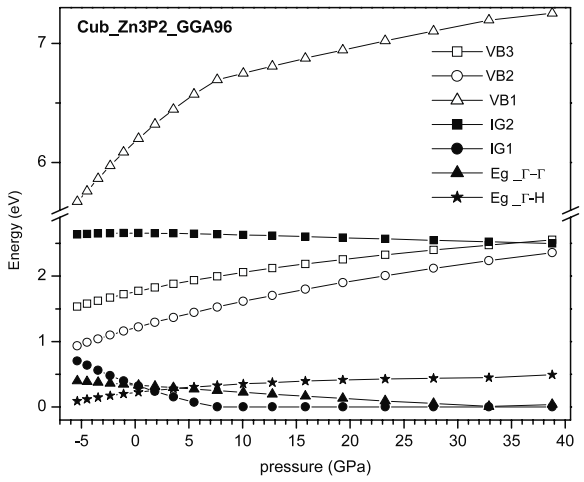

Figure 3. The behavior of the direct and indirect band-gaps (E_g), valence bandwidths (VB1, VB2 and VB3) and internal gaps (IG1 and IG2) for the cubic phase of Zn_3P_2 using GGA96 methods at different pressures.

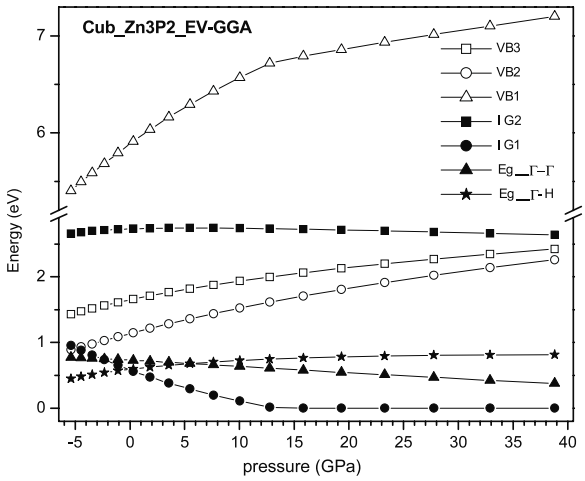

Figure 4. The variations of the direct and indirect band-gaps (E_g), valence bandwidths (VB1, VB2 and VB3) and internal gaps (IG1 and IG2) for the cubic phase of zinc phosphide using the EV-GGA approach at different pressures.

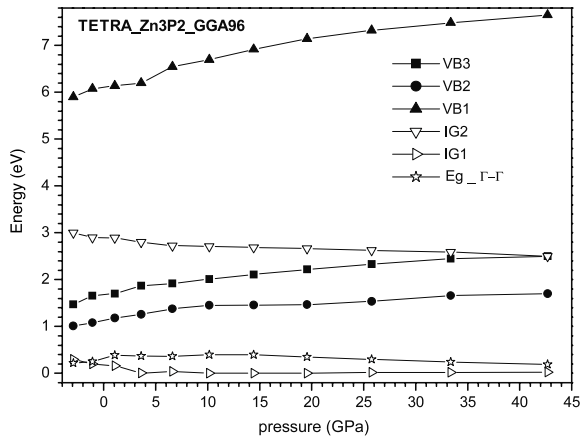

Figure 5. The behavior of the direct band-gaps (E_g), valence bandwidths (VB1, VB2 and VB3) and internal gaps (IG1 and IG2) for the tetragonal phase of zinc phosphide using the GGA96 approach at different pressures.

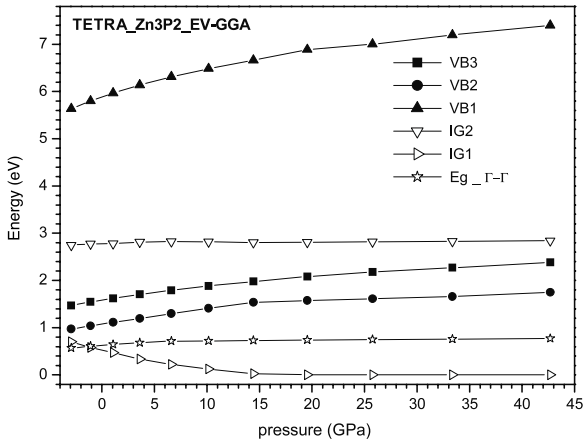

Figure 6. The variations of the direct band-gaps (E_g), valence bandwidths (VB1, VB2 and VB3) and internal gaps (IG1 and IG2) for the tetragonal phase of the Zn_3P_2 compound using the EV-GGA method at different pressures.

agreement as regards exchange energy. This approach, which is called the EV-GGA, has been applied to several solids and compared with other GGA based calculations [26, 28, 29]. It has been concluded that EV-GGA in general improves the band-gap and some other properties which mainly depend on the accuracy of the exchange–correlation potential, while for calculating the properties which are based on total energy calculations, such as the equilibrium lattice parameter and bulk modulus, usual GGAs are more appropriate. Hence, in the present work, first the equilibrium lattice constant and internal parameters are calculated by GGA96, and subsequently the results are applied to calculate the band structure of the Zn_3P_2 compound along high symmetry directions by EV-GGA and GGA96 for both phases at different pressures.

The calculated band structures at equilibrium theoretical lattice constants are presented as an example in figure 2. The valence bands for both phases are separated into three sub-bands that are labeled starting from the top as VB1, VB2 and VB3. The widths of these sub-bands are increased and the internal gaps (IG1, the energy gap between VB2 and VB1; IG2, the energy gap between VB3 and VB2) between them decreased by applying positive pressure. This behavior is consistent with the trend that smaller average bond lengths lead to stronger hybridization between different orbitals. The IG1 gap will be zero at pressures 7.63 and 15.84 GPa for the cubic phase and for tetragonal at 14.42 and 19.55 GPa respectively for GGA96 and EV-GGA methods. In the cubic phase, the type of band-gap (E_g) changes from Γ–H to Γ–Γ at pressure of 4.17 and 5.61 GPa respectively for GGA96 and EV-GGA but the band-gap of the tetragonal phase remains at Γ–Γ at all pressures. The effects of hydrostatic pressure on the behavior of band parameters such as band-gap, valence bandwidths and internal gaps are shown in figures 3–6 for both cases and both GGA96 and EV-GGA methods.

The values of band-gap for both GGA96 and EV-GGA decrease slowly on reducing the lattice parameter. Similar

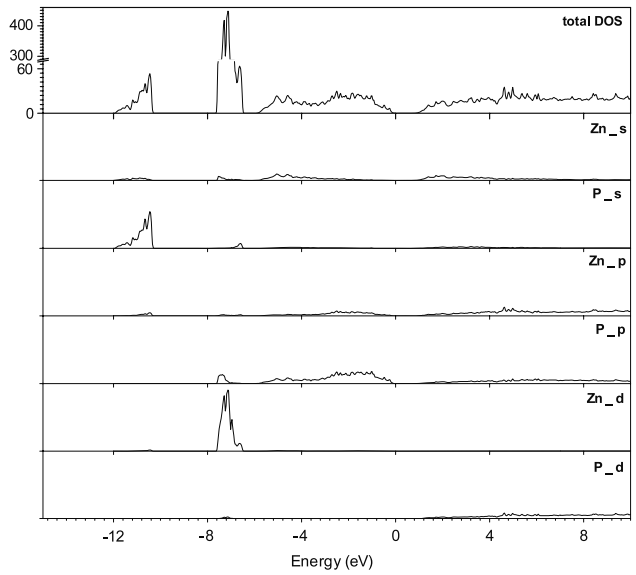

Figure 7. The total and partial density of states for s, p and d orbitals of the tetragonal phase of the Zn_3P_2 semiconductor compound calculated by EV-GGA at equilibrium lattice parameters.

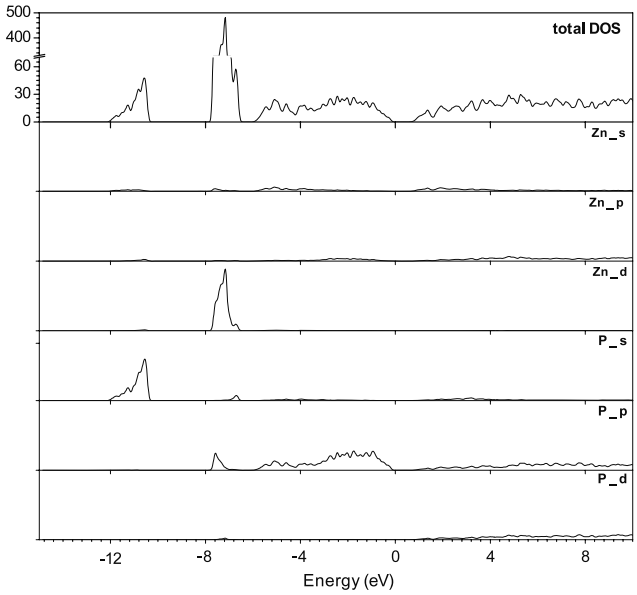

Figure 8. The total and partial density of states for s, p and d orbitals of the Zn_3P_2 semiconductor compound in the cubic phase, calculated by EV-GGA at equilibrium lattice parameters.

behavior is observed for the internal gaps. This means that, by applying pressure, the system is closer to the metal–insulator transition. At the theoretical equilibrium lattice constant, the band-gap values are obtained as 0.227 and 0.598 eV (Γ–H) for the cubic phase and 0.385 and 0.646 eV (Γ–Γ) for the tetragonal structure, using GGA96 and EV-GGA respectively.

It should be noted that, although GGA96 and EV-GGA estimate different values for the band-gap, the behaviors of the band-gaps with respect to positive pressure are rather similar.

The total and partial density of states are calculated by the tetrahedral method [30] using the EV-GGA exchange–correlation potential for both phases at zero pressure and are shown in figures 7 and 8. The VB3 group of sub-bands is mainly dominated by the s orbitals of P atoms. It is evident from DOS plots that the d orbitals of Zn atoms have the major contribution to the VB2 sub-bands. The s orbitals of zinc atoms and p states of phosphorus atoms are hybridized in the upper sub-bands.

4. Concluding remarks

The FP-LAPW + lo method has been applied to systematically study the structural and electronic properties of the Zn_3P_2 semiconductor compound in both cubic and tetragonal phases. To the best of our knowledge, no theoretical and experimental work has been done so far for the cubic phase, hence our results can serve as a prediction for future study. For the tetragonal phase, the obtained lattice constants and internal parameters are in good agreement with the available experimental data. For the cubic phase, at pressures of 4.17 and 5.61 GPa respectively for GGA96 and EV-GGA, the indirect band-gap changes to a Γ–Γ direct band-gap. Our calculations estimate that the tetragonal phase is more stable than the cubic.

Acknowledgments

The author acknowledges gratefully the Shahrekord University for encouragement and financial support. This work was carried out in the simulation laboratory of the physics department under project No 140-1020.

References

[1] de Carvalho M M G, Betinni J, Pudenzi M A A and Cardoso L P 1999 *Appl. Phys. Lett.* **74** 3669
[2] Gou H, Hou L, Zhang J, Wang Z, Gao L and Gao F 2007 *Appl. Phys. Lett.* **90** 191905
[3] Mokhtari A and Akbarzadeh H 2004 *J. Phys.: Condens. Matter* **16** 6063
[4] Mokhtari A 2008 *J. Phys.: Condens. Matter* **20** 135224
[5] Sieranski K, Szatkowski J and Misiewicz J 1994 *Phys. Rev.* B **50** 7331
[6] Misiewicz J 1990 *J. Phys.: Condens. Matter* **2** 2053
[7] Fagen E A 1979 *J. Appl. Phys.* **50** 6505
[8] Pawlikowski J M 1982 *Phys. Rev.* B **26** 4711
[9] Pawlikowski J M 1982 *J. Appl. Phys.* **53** 3639
[10] Misiewicz J 1989 *J. Phys.: Condens. Matter* **1** 9283
[11] Hermann A M, Madan A, Wanlass M W, Badri V, Ahrenkiel R, Morrison S and Gonzalez C 2004 *Sol. Energy Mater. Sol. Cells* **82** 241
[12] Bichat M, Pascal J, Gillot F and Favier F 2006 *J. Phys. Chem. Solids* **67** 1233
[13] Sathyamoorthy R, Sharmila C, Natarajan K and Velumani S 2007 *Mater. Charact.* **58** 745
[14] Pawlikowski J M 1985 *J. Phys. C: Solid State Phys.* **18** 5605
[15] Wyckoff R W G 1986 *Crystal Structures* 2nd edn, vol 2 (Malabar, FL: Krieger) pp 33–6
[16] Masumoto K, lsomura S and Sasaki K 1971 *Phys. Status Solidi* a **6** 515
[17] Nelson A J and Kazmerski L L 1990 *J. Appl. Phys.* **67** 1393
[18] Blaha P, Schwarz K, Madsen G K H, Kvasnicka D and Luitz J 2001 *WIEN2k, An Augmented Plane Wave + Local Orbitals Program for Calculating Crystal Properties* (Karlheinz Schwarz, Techn. Universität Wien, Austria), ISBN 3-9501031-1-2

[19] Hohenberg P and Kohn W 1964 *Phys. Rev.* **136** B864
[20] Kohn W and Sham L J 1965 *Phys. Rev.* **140** A1133
[21] Perdew J P, Burke K and Ernzerhof M 1996 *Phys. Rev. Lett.* **77** 3865
[22] Engel E and Vosko S H 1993 *Phys. Rev.* B **47** 13164
[23] Murnaghan F D 1944 *Proc. Natl Acad. Sci. USA* **30** 244
[24] van Schilfgaarde M and Harrison W A 1986 *Phys. Rev.* B **33** 2653
[25] von Stackelberg M and Paulus R 1935 *Z. Phys. Chem.* B **28** 427
[26] Dufek P, Blaha P and Schwarz K 1994 *Phys. Rev.* B **50** 7279
[27] Bachelet G B and Christensen N E 1985 *Phys. Rev.* B **31** 879
[28] Mokhtari A and Akbarzadeh H 2002 *Physica* B **324** 305
[29] Mokhtari A and Akbarzadeh H 2003 *Physica* B **337** 122
[30] Blöchl P E, Jepsen O and Andersen O K 1994 *Phys. Rev.* B **49** 16223